

We would like to thank both reviewers for their positive and useful comments on our m/s. The suggestion that we evaluate model performance in previous years turned out to be particularly valuable. It demonstrated that the assumption of normally distributed model errors (equation 3 in the original m/s), along with a small (and now corrected) error in processing lightning inputs, made it difficult for the model to capture previous high fires years within its posterior accurately. We felt that the ability of the model to reproduce the historical record, particularly in dry years, was a pre-requisite to applying the framework to assess meteorological influences over 2019 fires. As such, we have implemented a new error term to improve the model performance in previous extreme years. The most substantial revisions of the m/s with regard to this specific change are outlined below.

In the revised m/s, we now demonstrated that a logit-transformed, zero-inflated normal distribution is a much more appropriate way of representing the conditional probability of observation given parameter combinations, by including a new appendix Fig A1:

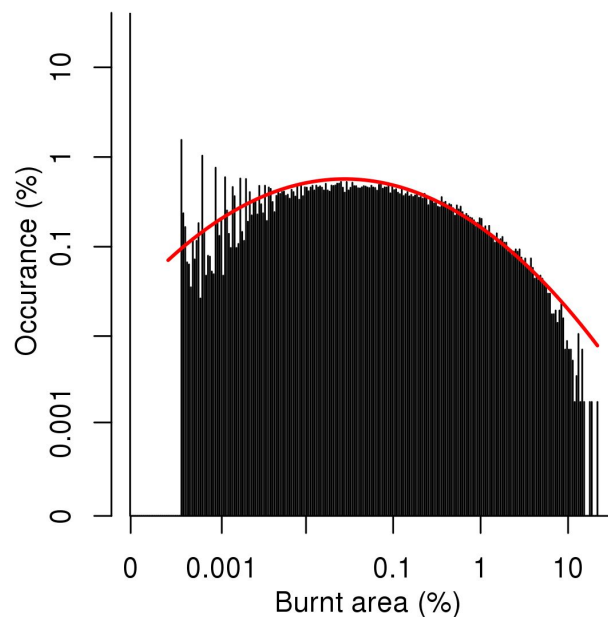


Figure A1: Distribution of burnt areas in MODIS Collection 6 MCD64A1 burned area product (Giglio et al., 2018) and (red line) fitted normal distribution for logit transformed burnt areas greater than 0.

We have also replaced our error description and the probability of observations given a parameter combination (lines 126-129) with:

41.47% of the burnt area observations are zero, and the remaining are normally distributed under *logit* transformation (Fig. A1). We, therefore, defined the likelihood, $P(Y_s | \beta)$, using a zero-inflated normal distribution on the logit transformed burnt area, as opposed to a simple normal distribution as used in Kelley et al (2019). This better described the observational to the simulated difference in burnt area during times of very low or very high burning. Our zero-inflation likelihood term is therefore described as:

$$P(Y_s = 0 | \beta) = 1 - BA_i^2 \times (1 - P_0)$$

$$P(Y_s > 0 | \beta) = [1 - P(Y_s = 0 | \beta)] \times \frac{N}{\sigma\sqrt{2\pi}} \exp \left\{ -\frac{1}{2} \sum_i^N \left(\frac{\text{logit}(y_i) - \text{logit}(BA_i)}{\sigma} \right)^2 \right\} \quad (3)$$

where i represents an individual data point, y_i is the burnt area observations, N is the observation sample size and $\text{logit}(x) = \log\left(\frac{x}{1-x}\right)$.

This new term allows for a much narrower uncertainty range at low burnt areas (see tan in the original and revised Figure 1) and, consequently, allows for a broader error term during periods of extreme burning. The models full posterior now captures levels of burning during historic dry years, as described by the response to reviewer #1s main comment.

The extra detail the model provides means we can focus on capturing drivers over smaller geographical areas. We have therefore modified our regions slightly to capture the west-east transect across the arc of deforestation in Brazil and to explain variations in burning throughout our area of active deforestation (AAD), though the AAD itself remains unchanged. We have therefore changed the region description (lines 154-161) to:

- A. Acre, Southern Amazonas States and Brazilian/Peruvian border
- B. Rondônia and Northern Mato Grosso, Brazil.
- C. Tocantins, Brazil,
- D. Maranhão and Piau in coastal deforestation regions
- E. Brazilian, Bolivian and Paraguayan border
- F. Area of Active Deforestation (AAD)
- G. [the areas of the AAD that is on] Southern end of agricultural-**humid tropical forest** interface in Brazil's central states, often associated with arc of deforestation in Brazil's central states
- H. [the areas of the AAD that is on] **Drier** savanna and woodland in Cerrado and Caatinga in the eastern Basin were land has already been heavily converted to agriculture
- I. [the areas of the AAD that is on] Southern **dry-deciduous** Chiquitano and Gran Chaco forests, mainly along the Amazon, La Plata watersheds.

See the response to reviewer #1 for all changes in relation to region descriptions.

We have split Figure 1 in two (i.e new Fig1. and Fig 2, with Fig. 2 and 3 in the original manuscript becoming 3 and 4). Notice the narrower posterior in tan and model performance compared to the original version

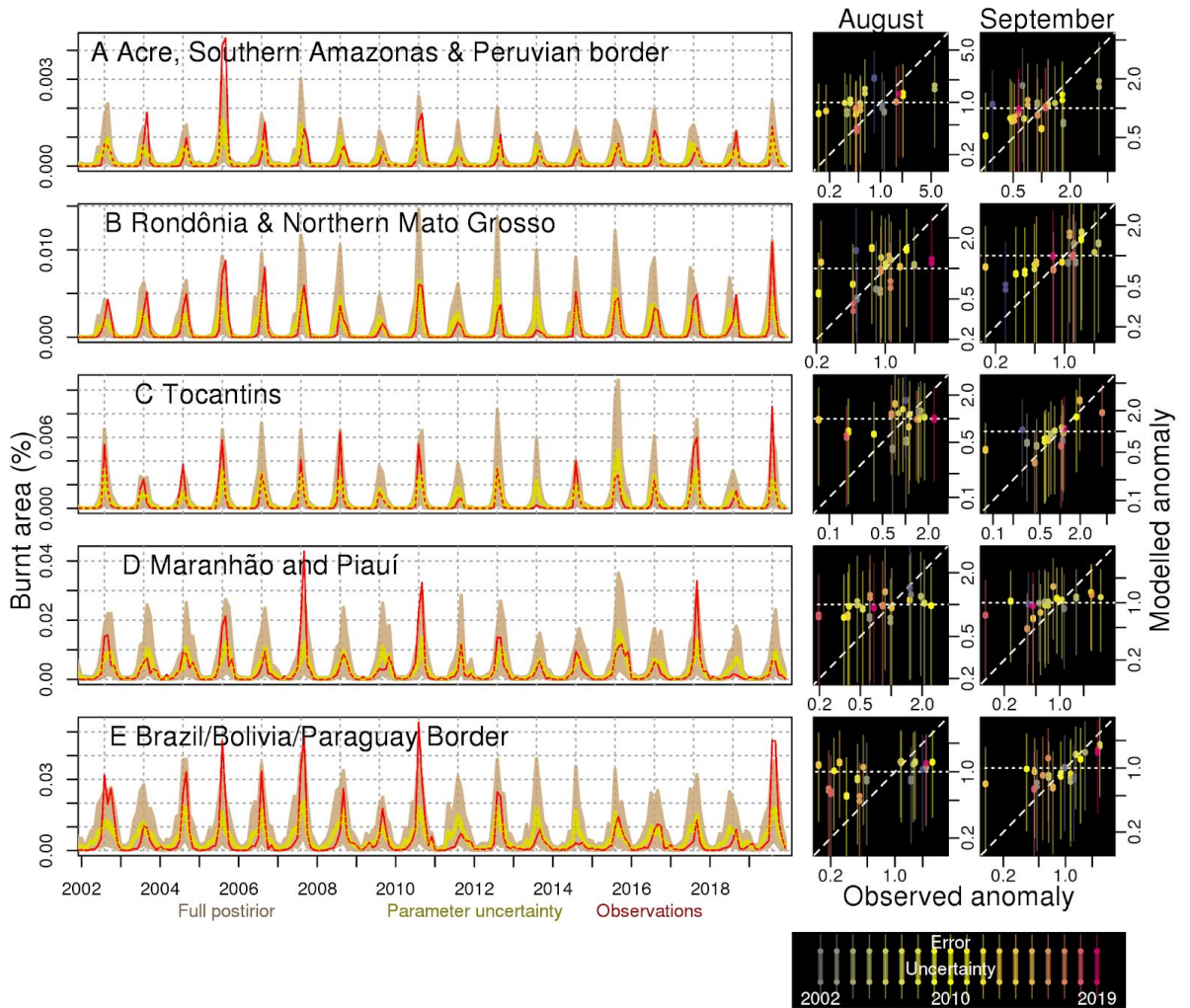


Figure 1: Time series and fire season anomalies for modelled and observed burnt area. See Fig. A2 for locations of A-R. Red lines show monthly burnt area observations from MCD64A1, yellow shows model accounting for parameter uncertainty (10-90%) and brown shows full model uncertainty (10-90%). The red line is dashed when observations and model accounting for parameter uncertainty overlap. Vertical grid lines are positioned for August each year. Right-hand plots show observed (x-axis) and modelled (y-axis) anomaly, calculated as 2019 burnt area over 2002-2019 climatological average burnt area for (first column) August and (second column) September. The colour indicates the year, with 2019 in red. Thin lines show 10-90% full model uncertainty, while dots and thick line indicate 10-90% parameter uncertainty

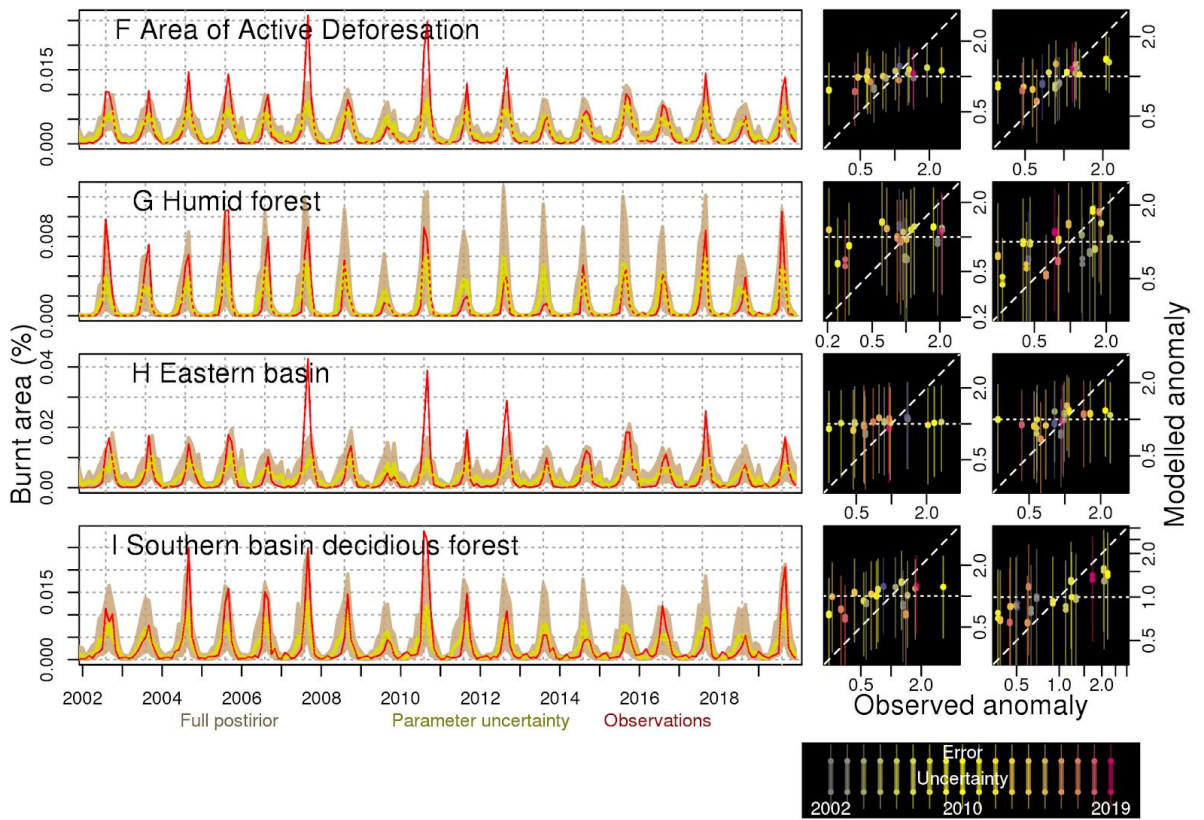


Figure 2: As Fig. 1, but for the “Area of Active Deforestation” region which incorporates areas where there has been a significant increase in agriculture and decrease in tree cover. See Fig. S4, and regions and increased agriculture and decreased tree cover in the (G) humid tropical forest, (H) savanna and (I) dry-deciduous Forest.

We also have modified the results and figures to capture these new insights (see attached revised m/s), though the overall conclusion of the paper - that meteorological conditions did not drive the increased burning in deforestation areas of South America in 2019, remain unchanged.